ISSN: 2455 - 9172

EIJO Journal of Engineering, Technology And Innovative Research (EIJO–JETIR)

Einstein International Journal Organization (EIJO)

Available Online at: www.eijo.in

Volume – 2, Issue – 2, March - April 2017, Page No. : 33 - 41

High Efficiency Ratio Bidirectional DC–DC Converter using Coupled Inductors

P.Saikiran, A.Arun Kumar, M.Praveen, Ch.Nithin Kumar

[1]B.Tech scholars, Dept of EEE, SVS Institute of Technology, Hanamkonda, Warangal, T.S, India

M. Pavan Kumar

[2]Assistant Professor, Dept of EEE, SVS Institute of Technology, Hanamkonda, Warangal, T.S, India

Abstract

In this paper, a high-conversion-ratio bidirectional dc-dc converter with coupled inductor is proposed. In the boost mode, two capacitors are parallel charged and series discharged by the coupled inductor. Thus, high step-up voltage gain can be achieved with an appropriate duty ratio. The voltage stress on the main switch is reduced by a passive clamp circuit. Therefore, the low resistance RDS (ON) of the main switch can be adopted to reduce conduction loss. In the buck mode, two capacitors are series charged and parallel discharged by the coupled inductor. The bidirectional converter can have high step-down gain. Aside from that, all of the switches achieve zero voltage-switching turn-on, and the switching loss can be improved. Due to two active clamp circuits, the energy of the leakage inductor of the coupled inductor is recycled. The efficiency can be further improved. The operating principle and the steady-state analyses of the voltage gain are discussed. Finally, a 24-V-input-voltage, 400-V-output-voltage, and 200-W-output-power prototype circuit is implemented in the laboratory to verify the performance.

Keywords: DC, Coupled Inductor, RDS, I/O-Put Voltage.

1. Introduction

Renewable energy systems are more and more widely used in the world such as solar and wind energy. However, photovoltaic (PV) solar or wind power cannot provide sufficient power when the load is suddenly increased. Thus, the battery with bidirectional dc–dc converter is needed [1]–[3]. Conventionally, the batteries are series strings used to provide a high voltage (HV).

However, temperature differences or little mismatches cause charge imbalance, which might shorten the life of batteries. Although the batteries operated in parallel strings alleviate the problems, the output voltage remains low by this connection way [4]. Therefore, a high-efficiency bidirectional dc–dc converter with a high convention ratio is a key component of battery applications [5]Isolated bidirectional dc–dc converters such as half- [6]– [9] and full-bridge types [10], [11] can provide high step-up and step-down voltage gains by adjusting the turn ratio of the transformer.

The high step-up gain and the high step-down voltage gain can be achieved. The number of switches is usually between four and eight. Also, some isolated bidirectional converters are characterized by a current-fed rectifier on the low voltage (LV) side and a voltage-fed rectifier on the HV side [12], [13]

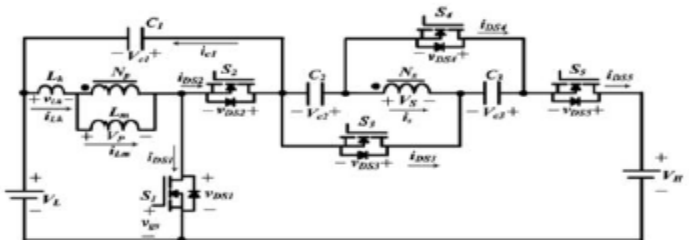

Figure 1: Circuit configuration of the bidirectional converter.

The switched-capacitor technique has proposed that parallel-charged and series-discharged capacitors can achieve high step-up gain. Also, series-charged and parallel-discharged capacitors can achieve high step-down gain. The character of the coupled inductor is that the secondary side can have opposite polarity when the switch is on and off. In the boost-state operation, this character is combined with the switched-capacitor technique. Two capacitors C2 and C3 are parallel charged when the switch is on and series discharged when the switch is off. In the buck-state operation, the coupled inductor is used as a transformer. Thus, two capacitors C2 and

*C*3 can be series charged by HV side and parallel discharged through the secondary side. In addition, the problem of the energy of the leakage inductor is also solved. In the boost-state operation, S_1 is the main switch, and capacitor C_1 recycles the energy. The voltage across switch S_1 can be clamped. Since switch S_1 has an LV level, the low conducting resistance $R_{DS(ON)}$ of the switch is used to reduce the conduction loss. In the buck-state operation, the main switches are S_2 and S_5. Two capacitors C_2 and C_3 with

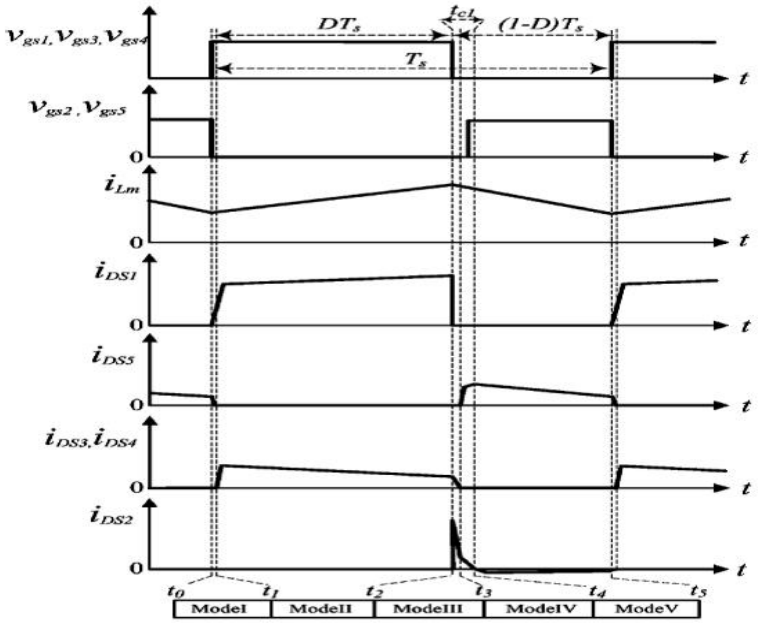

Figure 2: Key waveforms of the bidirectional converter in the boost state at the CCM.

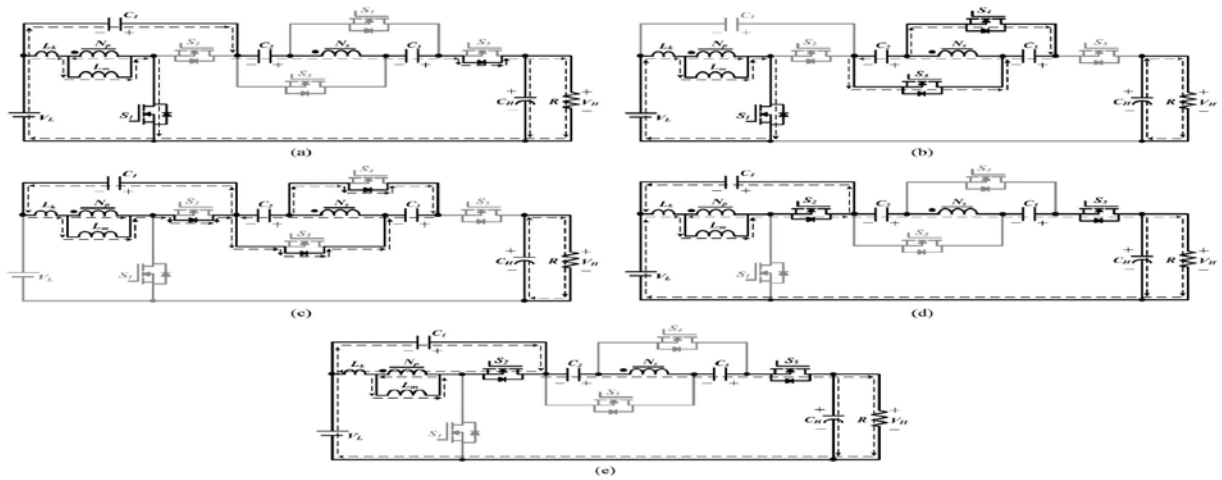

Figure 3: Current-flow path of the operating mode during one switching period in the boost state at the CCM. Modes (a) I, (b) II, (c) III, (d) IV, and (e) V.

Switches S_3 and S_4 are used as active clamp circuits, recycling the energy of the leakage inductor on the secondary side of the coupled inductor. Capacitor C_1 with switch S_2 is another active clamp circuit that recycled the energy of the leakage inductor on the primary side. Thus, four switches are ZVS turned on. The switching loss is improved; the efficiency can be increased. It is because that the high step-up converter needs a large input current, which results that the conduction loss is larger than the switching loss. Thus, reducing the switch voltage stress for alleviating the conduction loss and the elimination of reverse-recovery current is the key point to improve efficiency

2. Boost-state operation

According to the current of the coupled inductor, there are two operation modes; the first is the continuous conduction mode (CCM), and the second is the discontinuous conduction mode (DCM). Fig. 2 shows the typical waveforms in the boost state at the CCM, and Fig. 3 shows the current-flow path of the proposed converter at the CCM. Fig. 4 shows the typical waveforms in the boost state at the DCM, and Fig. 5 shows the current-flow path of the proposed converter at the DCM.

There are five operating modes in one switching period of the proposed converter in the CCM. Switches S_2, S_3, S_4, and S_5 are synchronous rectifiers. The main switch is S_1 for each mode. The operating modes at the CCM are described below.

1) Mode I [t_0, t_1]: At $t = t_0$, S_1 is turned on. S_2, S_3, and S_4 are off, and S_5 is on. The current-flow path is shown in Fig. 3(a). The voltage of the primary side is $V_L = v_{Lk} + V_p$. Thus, the leakage inductor L_k and the magnetizing inductor L_m are charged by the dc source V_L. Due to the leakage inductor L_k, the secondary-side current is linearly decreases. The reverse

2) Mode II [t_1, t_2]: S_1 is still on. S_2 and S_5 are off, and S_3 and S_4 are turned on at $t = t_1$. The current-flow path is shown in Fig. 3(b). The dc source VL charges the magnetizing inductor L_m, as well as the charging capacitors C_2 and C_3 via the coupled inductor. Voltages V_{c2} and V_{c3} are approximately equal to nV_L. Two capacitors are charged in parallel. The output capacitor C_H provides energy to load R. This operating mode ends when switch S_1 is turned off at $t = t_2$.

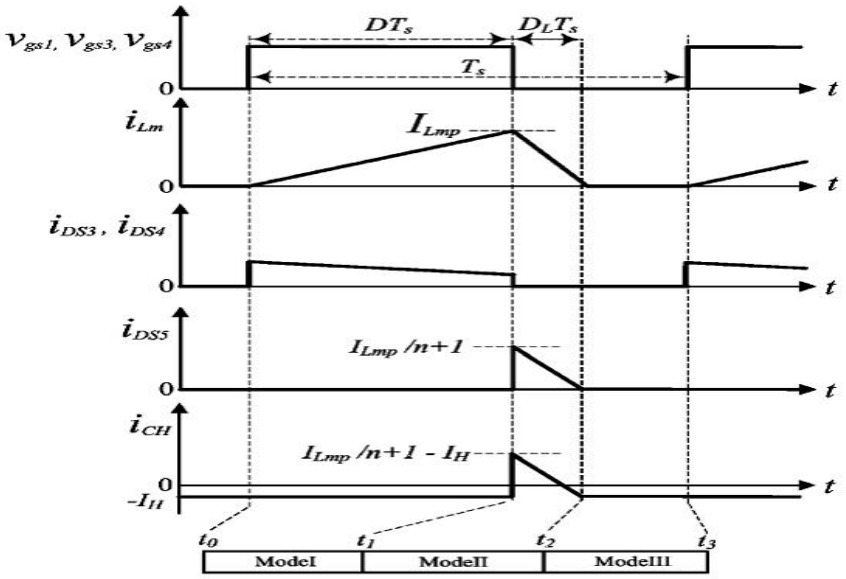

Figure 4: Key waveforms of bidirectional converter in the boost state at the DCM

3) Mode III [t_2, t_3]: During this time interval, S_1 remains turned off. The current-flow path is since the energy of L_m is depleted, C_H is discharged to load R. This mode ends when S_1 is turned on at $t = t_3$.

3. Buck-State Operation

In the buck-state operation, there are six operating modes in one switching period. Switch S_1 is the synchronous rectifier. The main switch is S_5. Switches S_2, S_3, and S_4 are auxiliary switches for achieving ZVS turn-on. Fig. 6 shows the typical waveforms, and Fig. 7 shows the current-flow path for each mode. The operating modes are described below.

1) Mode I [t_0, t_1]: At $t = t_0$, switch S_2 is off. The current flow path is shown in Fig. 7(a). Due to the leakage inductor L_k, the current of the secondary side of the coupled inductor flows through diode D_{s5}. Capacitors C_1, C_2, and C_3 are also discharged to V_H. Then, switch S_5 is turned on, and ZVS is achieved. Because of the HV V_H, current i_{DS1} and i_{DS5} linearly decrease. Meanwhile, the output capacitor C_L is charged by the magnetizing energy. When current i_{DS5} becomes zero at $t = t_1$, this operating mode is ended.

2) Mode II [t_1, t_2]: S_5 is on. The output capacitor C_L provides energy to load R. Capacitors C_1, C_2, and C_3, and the secondary side coil N_s are charged in series by HV V_H. Thus, the induced voltage V_p on the primary-side coil N_p makes current i_{DS1} decrease and charge the magnetizing inductor L_m. The magnetizing current i_{Lm} is increased. At $t = t_2$, current i_{DS1} is equal to zero. This mode is ended.

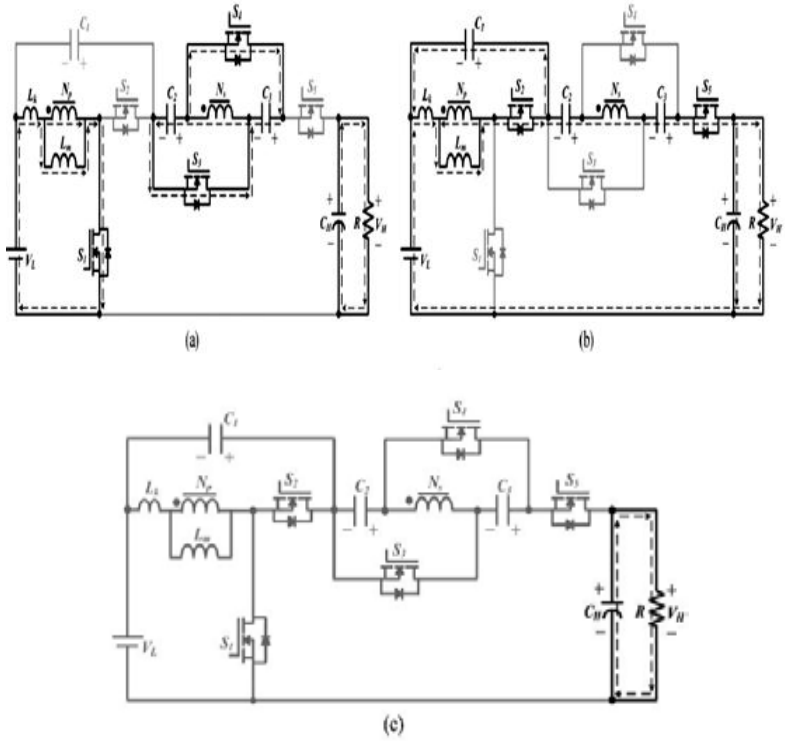

Figure 5: Current-flow path of the operating mode during one switching period in the boost state at the DCM. Modes (a) I, (b) II, and (c) III

3) Mode III [t_2, t_3]: S_5 is on. The current-flow path is shown in Fig. 7(c). At t = t_2, current i_{DS1} is equal to zero. The leakage inductor L_k is charged by the primary-side coil N_p. The charge current flows through the anti parallel diode D_{s2} of switch S_2. Then, S_2 is turned on, and ZVS is achieved. Capacitors C_1, C_2, and C_3, and the secondary side coil N_s are still charged in series by HV V_H, and the magnetizing inductor L_m is also charged. The output capacitor C_L provides the energy to load R. At t = t_3, i_{DS2} is equal to zero. This mode is ended.

4) Mode IV [t_3, t_4]: S_2 and S_5 are on. At t = t_3, capacitor C_1 starts to charge the magnetizing inductor L_m. The output capacitor C_L discharges to load R. Because two capacitors C_2 and C_3 and the coupled inductor are charged in series by the HV side V_H, the high step-down voltage gain can be achieved. At t = t_4, switches S_2 and S_5 are turned off. This mode is ended.

5) Mode V [t_4, t_5]: At t = t_4, switches S_2 and S_5 are turned off. The current-flow path is shown in Fig. 7(e). The current of the leakage inductor flows through the anti parallel diodes D_{s1}, D_{s3}, and D_{s4} of switches S_1, S_3, and S_4. Then, switches S_3 and S_4 are turned on, and ZVS turn on is achieved. The energy of the magnetizing inductor Lm discharges to capacitor CL and load R. At t = t_5, currents i_{DS3} and i_{DS4} are zero. This mode is ended.

6) Mode VI [t_5, t_6]: S_3 and S_4 are on. The current-flow path is shown in Fig. 7(f). At t = t_5, the energy of capacitors C_2 and C_3 discharges to the output capacitor C_L and load R through the coupled inductor. The magnetizing inductor L_m also discharges to the output. This mode is ended at t = t_6 when S3 and S_4 are off.

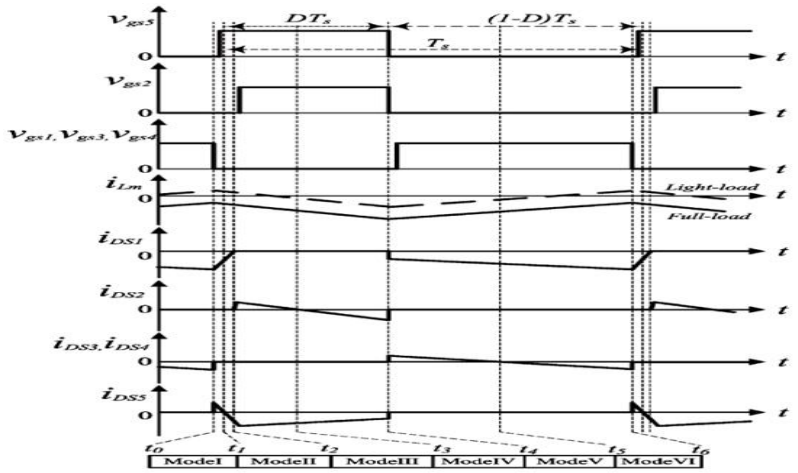

Figure 6: Key waveforms of bidirectional converter in the boost state at the DCM.

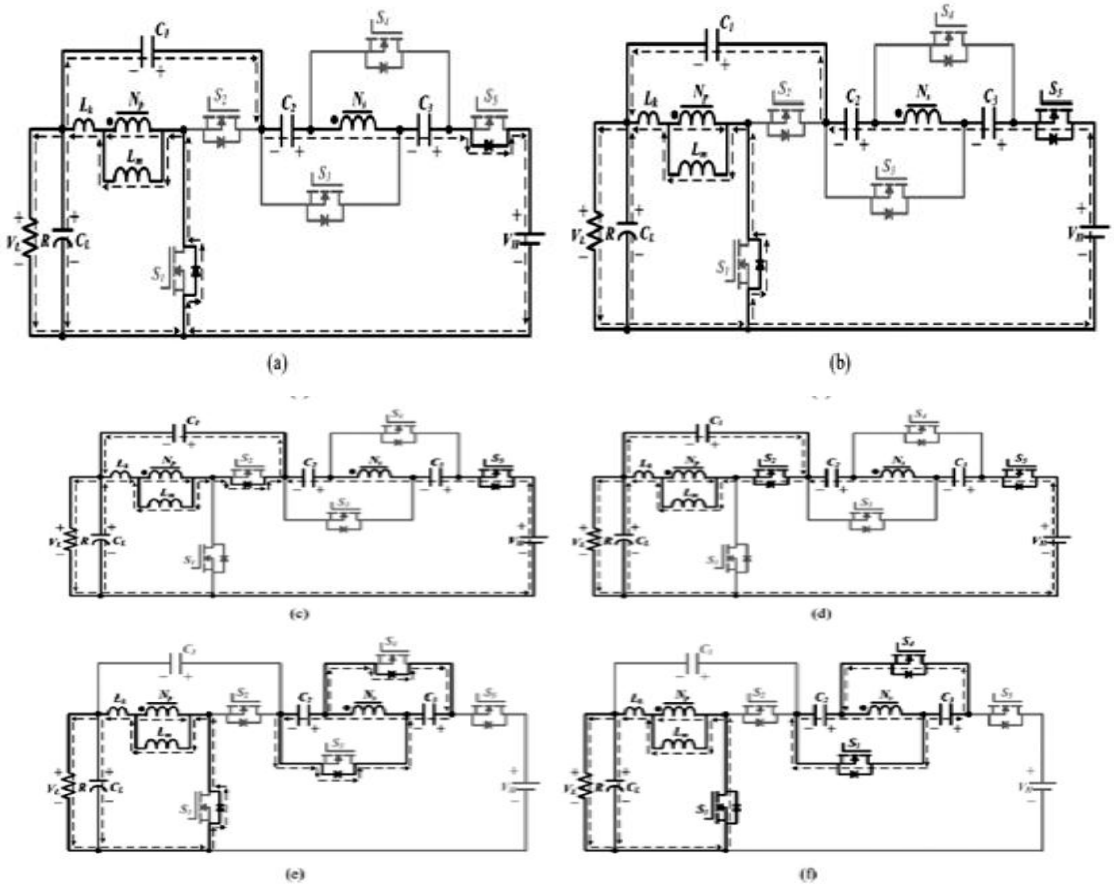

Figure 7: Current-flow path of the operating mode during one switching period in the buck state. Modes (a) II, (c) III, (d) IV, (e) V, and (f) VI) I, (b).

4. Simulation Model and Results

To demonstrate the performance and the functions of the proposed converter, a prototype circuit is implemented in the laboratory. The specifications are:

- DC voltage V_L and V_H: 24 and 400 V, respectively;
- Rated power: 200 W;
- Switching frequency: 50 kHz;
- Boundary condition: 100 W;
- MOSFETs S_1 and S_2: IRFP4568PBF; S_3-S_4: IXFK64N50P; S_5: IXFK64N60P;
- Coupled inductor: ETD-59, core pc40; N^p : N_s = 1: 5 L_m = 60μH; L_k = 0.16μH;
- Capacitors C_1: 47μF/100 V; C_2/C_3: 23.5μF.

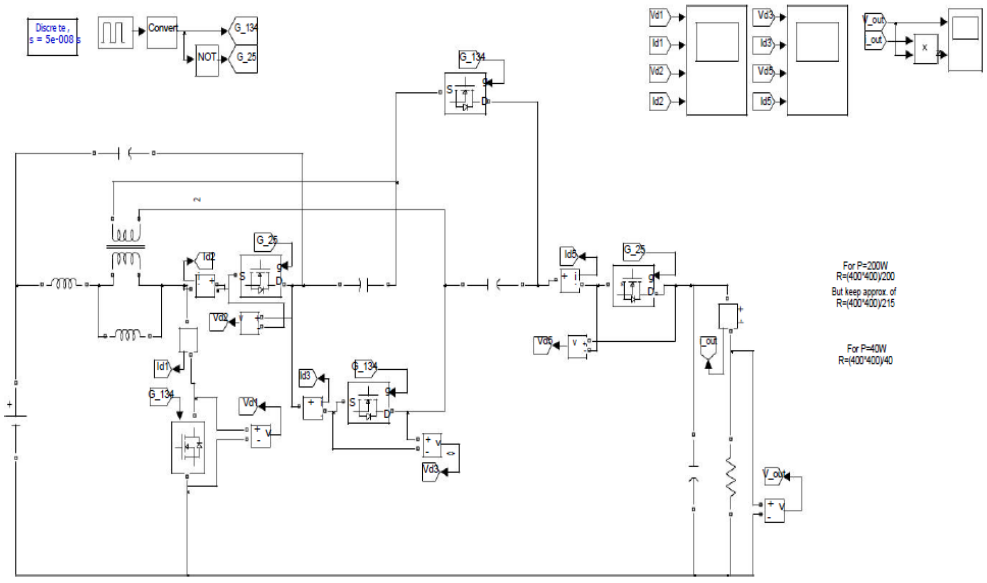

Figure 8: Simulation model for boost

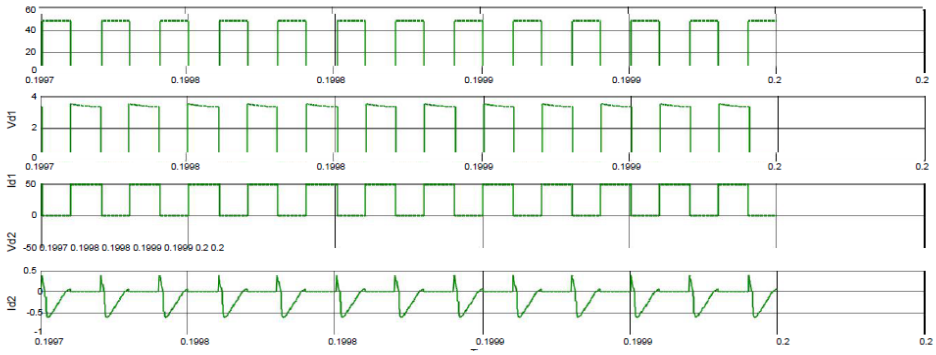

Figure 9: Simulation results in the boost mode under full load *P*o = 200 W.

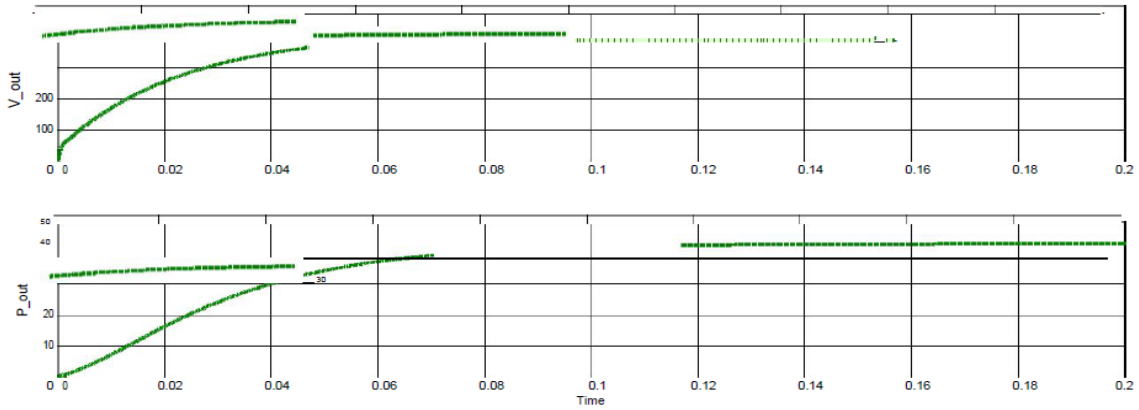

Figure 10: ZVS in the boost mode under 200 W.

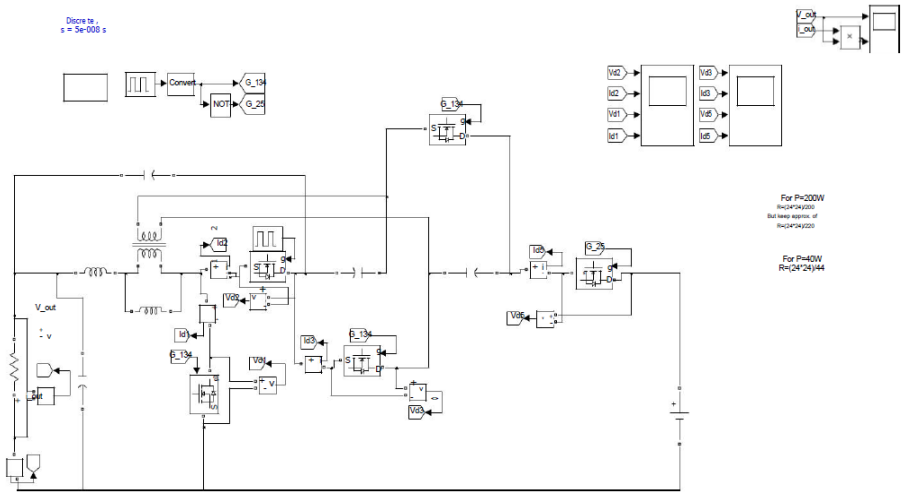

Figure 11: Simulation model for buck

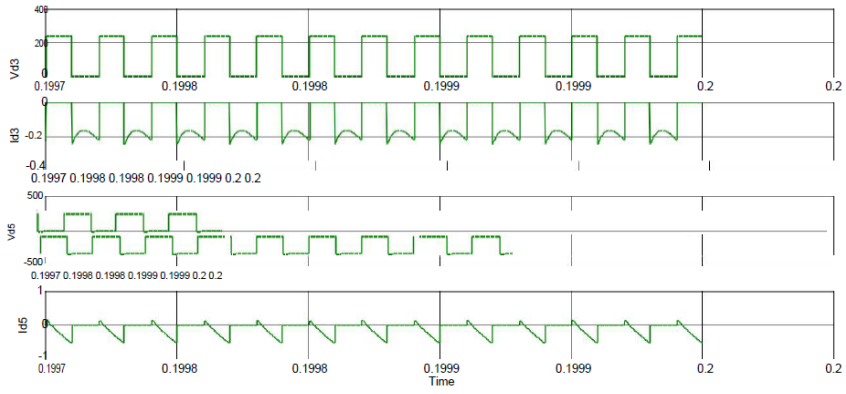

Figure 12: Simulation results in the buck mode under full load *Po* = 40 W.

5. Conclusion

This paper has proposed a novel, high-efficiency, and high step-up/step-down bidirectional dc–dc converter. By using the capacitor charged in parallel and discharged in series by the coupled inductor, high conversion ratio and high efficiency have been achieved. The steady-state analyses of the proposed converter have been discussed in detail. The voltage gain

and the utility rate of the magnetic core have been increased by using a coupled inductor with a low turn ratio. The energy of the leakage inductor has been recycled with the clamp circuit. A prototype circuit has been built in the laboratory. Simulation results show that the maximum efficiency is 97.33% at the boost mode and 96.23% at buck mode. This topology provides efficient conversion of various power sources. This technique can be also applied in different power conversion systems easily

6. References

[1] R. Gules, J. D. P. Pacheco, H. L. Hey, and J. Imhoff, "A maximum power point tracking system with parallel connection for PV stand-alone applications," IEEE Trans. Ind. Electron., vol. 55, no. 7, pp. 2674–2683, Jul. 2008.

[2] R. J. Wai, R. Y. Duan, and K. H. Jheng, "High-efficiency bidirectional dc–dc converter with high-voltage gain," IET Power Electron., vol. 5, no. 2, pp. 173–184, Feb. 2012.

[3] R. Y. Duan and J. D. Lee, "High-efficiency bidirectional dc–dc converter with coupled inductor," IET Power Electron., vol. 5, no. 1, pp. 115–123, Jan. 2012.

[4] R. J. Wai and R. Y. Duan, "High-efficiency bidirectional converter for power sources with great voltage diversity," IEEE Trans. Power Electron., vol. 22, no. 5, pp. 1986–1996, Sep. 2007.

[5] M. Jang and V. G. Agelidis, "A minimum power-processing-stage fuelcell energy system based on a boost-inverter with a bidirectional backup battery storage," IEEE Trans. Power Electron., vol. 26, no. 5, pp. 1568– 1577, May 2011.

[6] G. Ma, W. Qu, G. Yu, Y. Liu, N. Liang, and W. Li, "A zero-voltages witching bidirectional dc–dc converter with state analysis and soft switching- oriented design consideration," IEEE Trans. Ind. Electron., vol. 56, no. 6, pp. 2174–2184, Jun. 2009.

[7] F. Z. Peng, H. Li, G. J. Su, and J. S. Lawler, "A new ZVS bidirectional dc–dc converter for fuel cell and battery application," IEEE Trans. Power Electron., vol. 19, no. 1, pp. 54–65, Jan. 2004.

[8] H. Li, F. Z. Peng, and J. S. Lawler, "A natural ZVS medium-power bidirectional dc–dc converter with minimum number of devices," IEEE Trans. Ind. Appl., vol. 39, no. 2, pp. 525–535, Mar./Apr. 2003.

[9] B. R. Lin, C. L. Huang, and Y. E. Lee, "Asymmetrical pulse-width modulation bidirectional dc–dc converter," IET Power Electron., vol. 1, no. 3, pp. 336–347, Sep. 2008.

[10] K. Wu, C. W. de Silva, and W. G. Dunford, "Stability analysis of isolated bidirectional dual active full -bridge dc–dc converter with triple phase-shift control," IEEE Trans. Power Electron., vol. 27, no. 4, pp. 2007–2017, Apr. 2012.

[11] Z.Wang and H. Li, "A soft switching three-phase current-fed bidirectional dc–dc converter with high efficiency over a wide input voltage range," IEEE Trans. Ind. Electron., vol. 27, no. 2, pp. 669–684, Feb. 2012.

[12] F. Zhang and Y. Yan, "Novel forward-fly back hybrid bidirectional dc–dc converter," IEEE Trans. Ind. Electron., vol. 56, no. 5, pp. 1578–1584, May 2009.

[13] S. Jalbrzykowski, A. Bogdan, and T. Citko, "A dual full-bridge resonant class-E bidirectional dc–dc converter," IEEE Trans. Ind. Electron.,vol. 58, no. 9, pp. 3879–3883, Sep. 2011.